8-2023

Whitewater Sound Dependence on Discharge and Wave Configuration at an Adjustable Wave Feature

Taylor A. Tatum
University of Alabama

Jacob F. Anderson
Boise State University

Timothy J. Ronan
Earthscope Consortium

This document was originally published in *Water Resources Research* by Wiley on behalf of the American Geophysical Union:
Tatum, T.A., Anderson, J.F., and Ronan, T.J. (2023). Whitewater Sound Dependence on Discharge and Wave Configuration at an Adjustable Wave Feature. *Water Resources Research, 59*(8), e2023WR034554. https://doi.org/10.1029/2023WR034554

AGU ADVANCING EARTH AND SPACE SCIENCES

Water Resources Research

RESEARCH ARTICLE
10.1029/2023WR034554

Whitewater Sound Dependence on Discharge and Wave Configuration at an Adjustable Wave Feature

Taylor A. Tatum[1], Jacob F. Anderson[2], and Timothy J. Ronan[3]

[1]Department of Geography, University of Alabama, Tuscaloosa, AL, USA, [2]Department of Geoscience, Boise State University, Boise, ID, USA, [3]Earthscope Consortium, Washington, DC, USA

Key Points:

- For the first time, we examine combined effects of discharge and wave morphology on infrasound
- Monitorable infrasound is only produced above discharge rates exceeding ~35 m^3/s
- Wave morphology has potential to create powerful or insignificant infrasound, but interannual geomorphic changes may also be significant

Supporting Information:

Supporting Information may be found in the online version of this article.

Correspondence to:

T. A. Tatum,
taylortatum01@gmail.com

Citation:

Tatum, T. A., Anderson, J. F., & Ronan, T. J. (2023). Whitewater sound dependence on discharge and wave configuration at an adjustable wave feature. *Water Resources Research*, *59*, e2023WR034554. https://doi.org/10.1029/2023WR034554

Received 25 JAN 2023
Accepted 30 JUL 2023

Author Contributions:

Conceptualization: Jacob F. Anderson, Timothy J. Ronan
Data curation: Taylor A. Tatum, Jacob F. Anderson
Formal analysis: Taylor A. Tatum, Jacob F. Anderson
Funding acquisition: Jacob F. Anderson
Investigation: Taylor A. Tatum, Jacob F. Anderson
Methodology: Jacob F. Anderson
Resources: Jacob F. Anderson
Software: Taylor A. Tatum, Jacob F. Anderson
Supervision: Jacob F. Anderson
Visualization: Taylor A. Tatum
Writing – original draft: Taylor A. Tatum
Writing – review & editing: Jacob F. Anderson, Timothy J. Ronan

Abstract Stream acoustics has been proposed as a means of monitoring discharge and wave hazards from outside the stream channel. To better understand the dependence of sound on discharge and wave characteristics, this study analyzes discharge and infrasound data from an artificial wave feature which is adjusted to accommodate daily changes in recreational use and seasonal changes in irrigation demand. Monitorable sound is only observed when discharge exceeds ~35 m^3/s, and even above that threshold the sound-discharge relationship is non-linear and inconsistent. When sound is observed, it shows consistent dependence on wave type within a given year, but the direction of this dependence varies among the 3 years studied (2016, 2021, and 2022). These findings support previous research that establishes discharge and stream morphology as relevant controls on stream acoustics and highlights the complex, combined effects of these variables.

Plain Language Summary Previous research has explored the potential of using sound to measure stream discharge and evaluate stream hazards. Discharge and wave types were examined at an artificial wave feature that changes formation to adapt to daily changes in recreation and seasonal changes in irrigation. Through this study, we found that monitorable sound is only observed over a certain threshold and that the formation of the wave affects sound consistently during the year but changes between years, potentially due to outside effects on the overall stream. Future work should aim to better understand wave formation and specific wave traits that contribute to certain patterns of sound. Overall, this study supports the findings of previous research and applies them further by investigating the combined, complex effects of stream traits on sound.

1. Introduction

Analyses of rapids and other whitewater features in streams have shown that streams are capable of producing measurable sounds containing information on flow characteristics. Past research has found that sound power and spectrum depends on whitewater features' morphology (Ronan et al., 2017) and discharge (Osborne et al., 2021; Ronan et al., 2017; Schmandt et al., 2013). As more information is discovered about stream acoustics, potential applications for out-of-channel stream discharge gauges and the detection of increased drowning hazards can be further explored (Leutheusser & Birk, 1991), broadening the already growing list of acoustic monitoring used in earth and atmospheric processes. Geophysical acoustic monitoring focuses on infrasound (sounds whose frequencies are below 20 Hz, the human hearing limit) and low-frequency audible sounds (approximately 20–50 Hz) (Bedard & Georges, 2000). These sounds are frequently used to measure volcanic eruptions (Watson et al., 2022), snow and ice avalanches (Johnson et al., 2021), debris flows (Hübl et al., 2013), lahars (Bosa et al., 2021; Johnson & Palma, 2015), lava flows (Lyons et al., 2021), and nuclear explosions (Che et al., 2014). Because many of these research targets are currents, there is potential for overlap between the characteristics of water flows and other infrasound applications. In particular, lava flows have been shown to have breaking capabilities similar to water waves (Lyons et al., 2021). With further research, stream acoustics may be added to this list of monitoring applications.

1.1. Hydraulics of Breaking Waves in Streams

The breaking of buoyancy waves in water, characterized by turbulence and air entrainment that create the characteristic whitewater appearance, is widely recognized as a source of seismoacoustic generation (Lyons et al., 2021; Osborne et al., 2021; Ronan et al., 2017). In gravity-dominated processes like open-channel flow and buoyancy waves, an important descriptor of flow characteristics is the dimensionless Froude number

$$\mathrm{Fr} = v / \sqrt{gh} \quad (1)$$

where v is flow speed, g is the acceleration due to gravity (9.8 m^2/s), and h is the depth of the flow.

In flowing channels, stationary breaking waves called hydraulic jumps form where water transitions from supercritical flow (Fr > 1) to subcritical flow (Fr < 1). In uniform channels, hydraulic jump morphology corresponds to a range of Froude numbers of the incoming supercritical flow. For example, undular jump morphology is associated with a Froude number from 1.0 to 1.7, while weak breaking hydraulic jump morphology is associated with Froude numbers from 1.7 to 2.5 (Chow, 1959). Fr = 1.7 represents a boundary between undular jumps that turn to weak breaking hydraulic jumps, which creates a collapsing wave that transfers kinetic energy to associated seismoacoustic fields (Ronan et al., 2017). Additionally, the collapsing and breaking of ocean waves within the shoreline has been associated with infrasound generation; research suggests there may even be a positive correlation between signal and wave height (Arrowsmith & Hedlin, 2005). Hydraulic jumps identified in high-speed lava flows have even been identified as a source of infrasound (Lyons et al., 2021).

Acoustic generation has also been linked to stream morphology, including features such as bed roughness, obstacles within the stream (Osborne et al., 2021), and drops that form hydraulic jumps (Ronan et al., 2017). At geomorphic features like weirs (Leutheusser & Birk, 1991) or downward steps in the streambed (De Padova et al., 2017), hydraulic jumps are dependent on surrounding stream variables such as depth of flow, stream slope, and artificial obstructions, making these features more complicated than in uniform channels. As such, they are categorized morphologically following different schemes. The categories used for steps, ranging from A-jumps that occur at very high tailwater depth, to wave jumps and wave trains at intermediate tailwater depth, to B-jumps at low tailwater depth, are most relevant to our study site. The wave setting at our study site labeled "Green Wave" (Figure 2b) resembles the "wave jump" condition (De Padova et al., 2017; Figure 2c), and the wave setting labeled "Wave/Hole" (Figure 2e) resembles the "minimum B-jump" condition (De Padova et al., 2017; Figure 2f).

1.2. Benefits of Using Infrasound to Measure Stream Flow

Infrasound is an established tool for monitoring a variety of flow phenomena in or adjacent to the atmosphere. In particular, atmospheric sound from fluvial origins has been studied from lahars (Bosa et al., 2021; Johnson & Palma, 2015) and waterfalls (Johnson et al., 2006). We consider low-frequency sound as an appealing monitoring method for several reasons: it can be measured remotely, its low data rate makes automated real-time analysis feasible and computationally inexpensive, it doesn't require human supervision to operate and needs infrequent maintenance, and it is not affected by loss of visibility (e.g., darkness, fog, etc.).

Continuous stream monitoring is currently performed by in-stream gauges that measure river stage, from which discharge is estimated using an empirical rating curve. Stream gauges are declining in number and distributed unevenly (e.g., low-order streams and the global south are under-monitored) (Fekete & Vörösmarty, 2007; Hannah et al., 2011). A common issue found during flooding periods (where recorded data is often the most important) is that in-stream gauges along heavily flooded stream systems are often destroyed; this forces researchers to reconstruct and estimate peak flows for these events and deprives monitoring agencies of critical data during flood emergencies (Gochis et al., 2015). By comparison, we propose infrasound as a potentially cheaper, non-invasive, and less flood-prone supplement or alternative to continuously monitor river stage. Low-cost infrastructure would allow gaps in hydrometric stations to be filled, and the out-of-stream placement of infrasound sensors would allow better protection for equipment. The prospect of using infrasound for monitoring discharge motivates research of how a stream feature's discharge-sound relationship is affected by morphology so that gauging sites can be selected where sound characteristics correspond to discharge unambiguously. Infrasound monitoring could also enable monitoring of hazardous wave conditions. At certain combinations of discharge and tailwater height, hydraulic jumps at weirs or drops in streams can partly submerge, forming a rotating current with a strong upstream-directed surface current. Though their whitewater is visually less impressive than non-submerged hydraulic jumps, these vortices are much more dangerous because buoyant objects, recreators, and rescuers can become trapped in the turbulent back-current that even strong swimmers cannot escape (Leutheusser & Birk, 1991). An improved understanding of how wave morphology affects infrasound production could enable automated alerts to recreators and safety personnel when changing flow conditions create hazards like submerged jumps, potentially helping save lives.

10.1029/2023WR034554

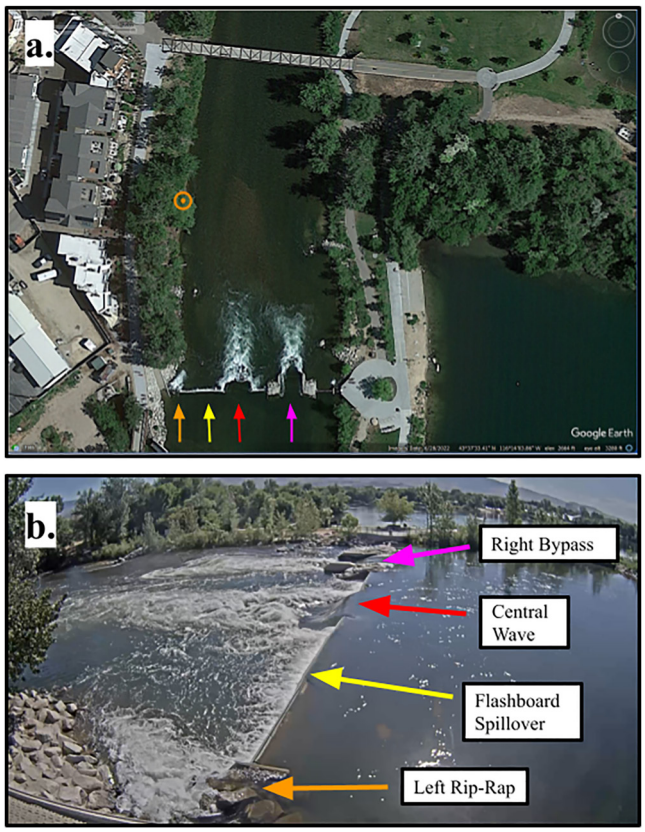

Figure 1. (a) Satellite view of the site (28 June 2022), with the recording site signified by a orange dot and (b) webcam view of the site (27 June 45 m^3/s), with each of the four flow paths through the dam marked. The left-most rip-rap is marked with an orange arrow, the flashboard spillover with a yellow arrow, the main central wave with a red arrow, and the right-opening with a magenta arrow.

2. Methods

In this study, we investigate the relationship between sound, discharge, and wave configuration at an artificial, adjustable dam located in Boise, Idaho (USA) known for adjustments in configuration relating to daily, weekly, and seasonal changes in recreational and irrigation demand. This study measures both low-frequency audible sound (20–50 Hz) and infrasound (<20 Hz); in the context of this paper we use the term "infrasound" broadly to include all acoustic signals recorded. Using infrasound recordings from 2016, 2021, and 2022, we analyzed the effects of discharge and dam configuration on the acoustic spectrum on daily and seasonal scales in order to better understand the relationships between infrasound and stream features with the intent to further explore potential applications in stream monitoring.

2.1. Site Description

This study focuses on an adjustable dam, commonly referred to as Boise Whitewater Park Phase 1 (BWPP1). Flashboards and Wave Shapers (Figure 2, orange and red features, respectively) located within the dam determine the shape of the wave by controlling the angle of entry and speed of water allowed to pass. Park operators adjust flashboards and waveshapers, to create appealing waves for recreation and maintaining required irrigation diversions while adapting to seasonal changes in discharge and interannual changes in riverbed morphology due to sediment erosion and deposition (City of Boise, 2022).

At BWPP1, water is allowed to flow through the dam in one of four ways: a small, non-adjustable spillway on river left partly obstructed by rip-rap, the main, central adjustable wave a bypass operated as safe passage for boats on river right, and any additional water that spills over the flashboards (Figure 1). For the purpose of measuring infrasound, this study assumes that the central wave is the dominant infrasound source, as both the rip-rap on the left and bypass on the right lack large waves. The rip-rap on the left side of the river is relatively small in area and by dissipating hydraulic power piecemeal, reduces the water's ability to form a strong energy dissipator that would be expected to generate infrasound. While the right bypass sometimes creates foam trails that reach the same distance away from the dam as the whitewater from the central wave, by design the right opening is intended to create a gentle outflow for safe passage, which we also consider less likely to make infrasound. When present in

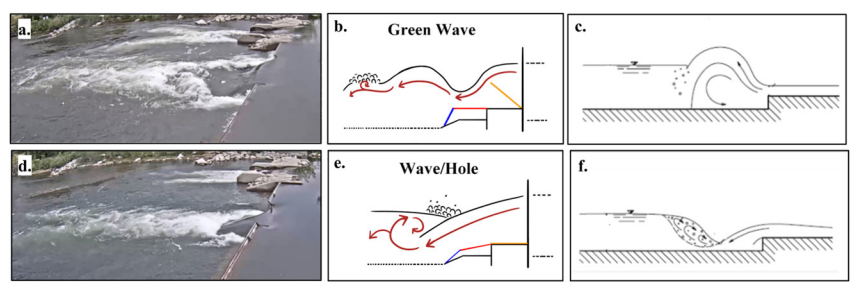

Figure 2. Images (taken 11 June 2022 (a) (~35 m^3/s) and 9 June 2022 (b) (~15 m^3/s)) and cross-section drawings of (a, b) Green Wave and (d, e) Wave/Hole configurations, included related figures of hydraulic jump formations from De Padova et al. (2017) (c, f). Flashboards (orange) are adjusted by pneumatic bladders that range over a variety of angles (including the ability to completely block flow through sections of the dam), while hydraulic-controlled wave shapers (red) range only between 0° and 9°. Green Waves have smooth fronts and are formed by water spilling over elevated flashboards onto horizontal waveshapers, while Wave/Hole are circulating waves with foamy, turbulent fronts formed by water that is allowed to plunge into the downstream pool by horizontal flashboards and downward-sloped waveshapers. The blue "trash gates" prevent debris accumulation under the waveshapers and do not significantly affect flow patterns.

our data, spillover makes up a small portion of discharge flowing through the dam, but previous research at this site has shown that large amounts of spillover can create powerful infrasound (Ronan et al., 2017), so we consider the possibility that water spilling over the flashboards may contribute meaningfully to our recorded infrasound. Though our recording site was closer to the left side of the dam than the right side (Figure 1), due its long distance downstream from the wave the resulting detection bias on possible infrasound sources is small (power ratio vs. the main wave feature less than 1.5). Therefore, any major infrasound produced along any part of the dam would have been detectable.

BWPP1 produces two types of wave configurations: Green Wave and Wave/Hole (Figure 2). They differ in their retentiveness, a term used by the whitewater recreation community to describe the tendency of a wave to block the passage of floating objects. Green Waves typically have smoother fronts with relatively little whitewater at the surface (Asiaban et al., 2021); Wave/Holes have abrupt, recirculating fronts with whitewater at circulating points. These descriptions pertain to the initial wavefront at the hydraulic jump itself, and any subsequent downstream waves may be different. BWPP1 alternates between these two configurations for recreational use with schedules that vary throughout the flow season. During periods of high flow (>∼60 m^3/s), additional flashboards are opened to allow higher volumes of water to pass through, which overrides any prior wave configuration schedule. Because of their morphological differences, we marked these days as not following either green wave or wave/hole conditions (Text S1 in Supporting Information S1).

2.2. Field Methods and Data Analysis

We installed Gem Infrasound Loggers (Anderson et al., 2018) along the left bank of the Boise River during the 2016, 2021, and 2022 flow seasons. The Gem samples at 100 samples per second and has a flat response between 0.039 and 27.1 Hz (−3 dB corner frequencies). At frequencies greater than 1 Hz, the Gem's self noise falls between the IMS low and medium noise models (Brown et al., 2014); specifically, within the 10–50 Hz band, the self noise power is $8.4 * 10^{-6}$ Pa^2 root-mean-square. This site was instrumented ∼46 m downstream of the dam; we only used one sensor in 2016, but in 2021 and 2022 an additional sensor was installed for redundancy. During the 2022 flow season, photos of the wave were taken of the site through webcams provided by the park and used to describe wave morphology. Discharge data for all 3 years were retrieved from USGS gauge #13206000 (U.S. Geological Survey, 2016) located 5.26 km downstream; discharge at this site was expected to be the same as BWPP1 except for an approximately 1-hr delay and small flow differences from minor ungauged irrigation diversions and returns. During the periods studied (excluding flood conditions, which are not interpreted), discharge was not sufficient to transport bedload cobbles and gravel.

Maximizing signal fidelity is essential when studying low-power continuous signals, and we took various actions in the field and in analysis to achieve this. Sensors were concealed along a wooded section of the river bank; the site's protection from wind helped reduce noise from atmospheric turbulence without impeding the infrasound. During analysis, hour-long windows were selected during the early morning hours local time (9:00–10:00 UTC) to minimize background noise from human activity and atmospheric turbulence. Stationary river and wave conditions are expected at this time because park staff, irrigation officials, and upstream reservoir managers do not normally make changes overnight. Additionally, inspection of all data showed that infrasound frequencies below 10 Hz were never associated with flow conditions in the park, and instead were dominated by transient atmospheric turbulence noise or, in quiet conditions, by instrument self-noise. Therefore, after deconvolving the sensor's instrument response, we filtered all data above 10 Hz to remove noise without affecting signals of interest. We calculated spectra using Welch's method, which, by dividing the hour-long recording period into 10-s windows with 50% overlap and averaging all spectra, ensures that the resulting spectrum is representative of the recording period and is not strongly influenced by occasional transients.

3. Results

This study investigates stream discharge, infrasound power, and infrasound frequency. Figures in this paper are divided into three sections to demonstrate three different variables: (a) stream discharge from the nearest USGS gauge, (b) infrasound power, and (c) infrasound spectrogram. Infrasound power is the mean of squares of the filtered infrasound pressure signal, a single value for each day's hour-long recording period. Spectrograms show how the power during each recording period is distributed over frequency. Bright-colored horizontal bands in the

spectrogram represent frequencies that consistently have high power over long periods of time; narrow horizontal bands are often produced by building air conditioners and other large machines. Bright-colored vertical bands in the spectrogram indicate moments in time that have monitorable power at a wide range of frequencies, most commonly due to storms.

3.1. Infrasound Over the 2021 and 2022 Flow Seasons

Figure 3 shows stream discharge, infrasound power, and infrasound frequency during 2021 and 2022. Discharge in 2021 ranges from ~10 to 50 m^3/s, while discharge in 2022 ranges from ~10 to 80 m^3/s. For the context of this project, we will be examining discharge below the threshold of ~60 m^3/s, where the dam is set to a different high-flow configurations. In 2021, large peaks in infrasound power occur simultaneously with the year's highest discharges (~50–55 m^3/s). By contrast, in 2022, the highest values of infrasound power occur after the flow drops from a peak of 80 to a plateau around 40 m^3/s. Outside of these high flow periods, changes in infrasound power (ranging from 2 to 4 * 10^{-4} Pa^2) do not coincide with changes in discharge or wave configuration; these fluctuations are likely noise.

3.2. Daily Changes During 2016, 2021, and 2022 Flow Season

We investigate day-to-day changes in infrasound over select periods including high flows during 2016, 2021, and 2022 to determine the effects of wave configuration. The selected periods include May 2016, May–June 2021 (Figure 5), and June–August 2022 (Figure 6, which also includes images for select days during that period). In 2016, 2021, and 2022, dominant frequencies were consistently between 15 and 35 Hz on days with monitorable infrasound, regardless of wave configuration or discharge; monitorable fluvial infrasound only occurs at discharges above 35 m^3/s, regardless of the year (Figure 4). For discharge less than 35 m^3/s, spectra are similar between green wave and wave/hole days, suggesting that the spectra are dominated by local ambient noise other than the river. We attribute sharp peaks in the spectrum, including 18, 30, and 45 Hz, to anthropogenic noise (probably mechanical systems in nearby buildings). For discharge greater than 35 m^3/s, spectra are much more powerful than below 35 m^3/s, and the green wave ($N = 31$) and wave/hole ($N = 11$) spectra are easily distinguished, with the green wave spectrum considerably more powerful at all frequencies. All recorded infrasound spectra exceed the infrasound logger self-noise at all frequencies in the band of interest (>10 Hz), indicating that the primary limitation to detecting river infrasound at this site is ambient environmental noise rather than the instrument's self-noise. *t*-tests were run to determine if wave morphology had a effect on power above and below 35 m^3/s; results show the visually apparent difference between green waves and wave/holes to be significant for discharge above 35 m^3/s were observed to be significant ($p < 0.05$), whereas results for discharge below 35 m^3/s, the difference in sound power between green wave and wave/hole was insignificant ($p > 0.05$).

In 2016, a distinct dependence of infrasound power on wave configuration was observed in the first week (3 and 10 May) when discharge was approximately 42 m^3/s (Figures 4a and 4b). During this week, Green Wave configuration days have much lower acoustic power than Wave/Hole configuration days. A similar difference in wave configurations was also observed in the third week of June 2022 (19 and 26 June) and the second and third week of July 2022 (13 to 19 July) when discharge was approximately 42–45 m^3/s (Figures 5j and 5k). However, the opposite pattern was observed in 2022, where Green Waves displayed a higher acoustic power than Wave/Hole configurations. On the other hand, no dependence of acoustic power on wave configuration was observed during 11–23 May 2016 (when discharge varied from 45 to 80 m^3/s) (Figures 4a and 4b) and in all 2021 data (with a maximum discharge of 55 m^3/s) (Figures 4d and 4e).

Images taken throughout June and July 2022 also display a similar lack of dependence. Most days maintain similar, recognizable Green Wave and Wave/Hole configurations that continue to be observed throughout the flow season. Images shown in Figure 4 include a range of days from low to medium discharge (~15–40 m^3/s). Certain days (Figures 5d, 5e, 5h, and 5i) display patterns of medium infrasound power Green Wave configuration paired with a low power Wave/Hole configuration at the same, similar level of discharge (~35–40 m^3/s).

4. Discussion

4.1. Dependence of Infrasound on Discharge

Monitorable infrasound power only occurs at discharge rates above 35 m^3/s; sound below this threshold is attributed to noise (Figure 4). Background noise can often be attributed to atmospheric turbulence and human activity–mainly mechanical systems (e.g., heating, ventilation, air conditioning, and refrigeration) from nearby buildings.

10.1029/2023WR034554

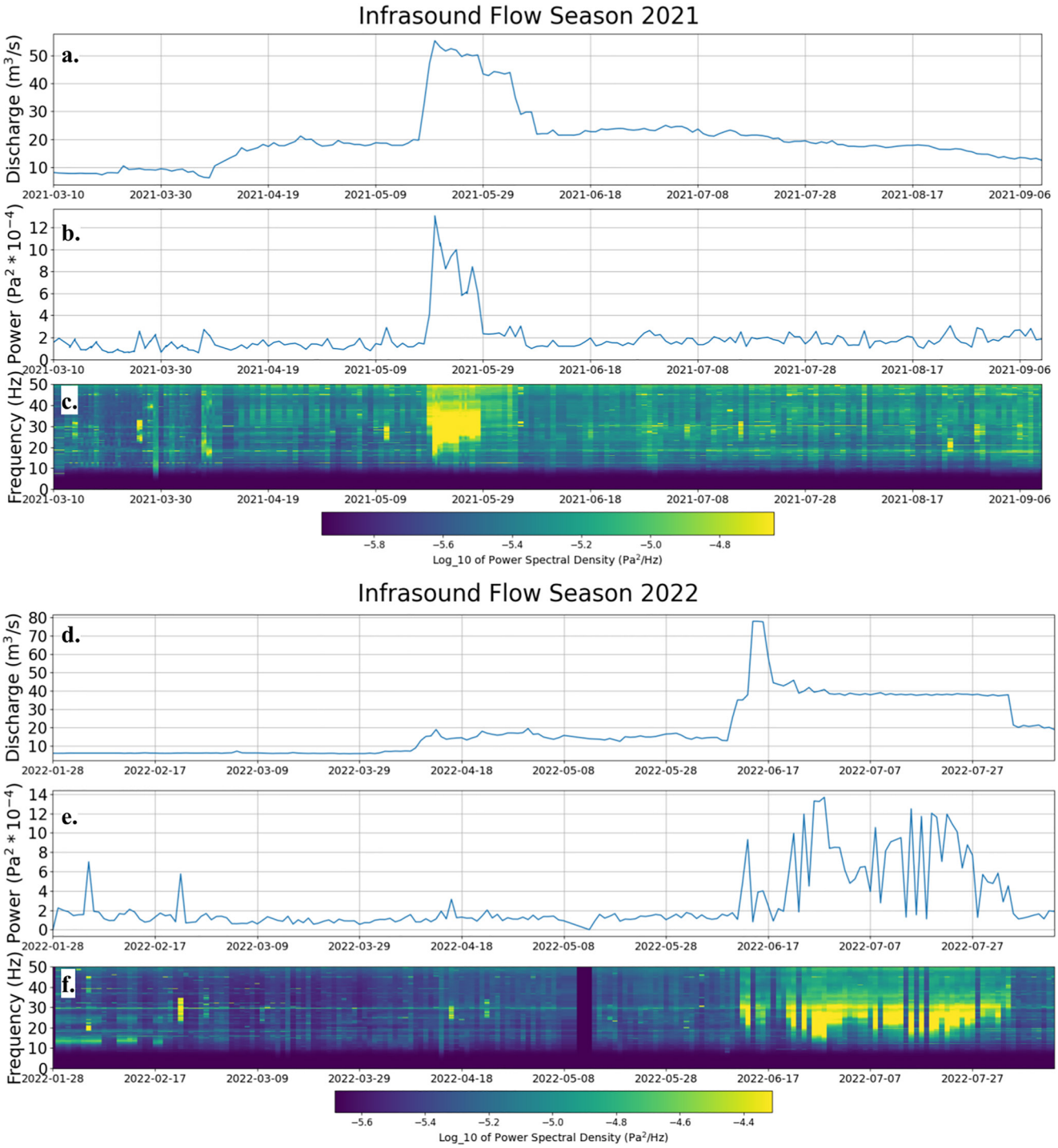

Figure 3. (a, d) Discharge, (b, e) Power, and (c, f) Frequency of stream and infrasound data recorded from March–September 2021 to January–August 2022. Periods of increased infrasound power in February and early March 2022 (18 February through 6 March) are related to construction near the dam.

An example of this background noise can be seen in Figure 2f, where there is a faint but constant ~30 Hz tone found throughout the duration of the year; this same frequency can also be spotted in early June in Figure 5l. This is also shown in Figure 4, where sharp peaks in the spectrum (18, 30, and 45 Hz) are attributed to background noise. We attribute spikes in infrasound frequency near 10 Hz to construction machinery working near the dam, and high power at a wide range of frequencies to stormy weather. These noise types are familiar in infrasound studies and not surprising to see at BWPP1. The 35 m^3/s threshold for infrasound production was observed in all

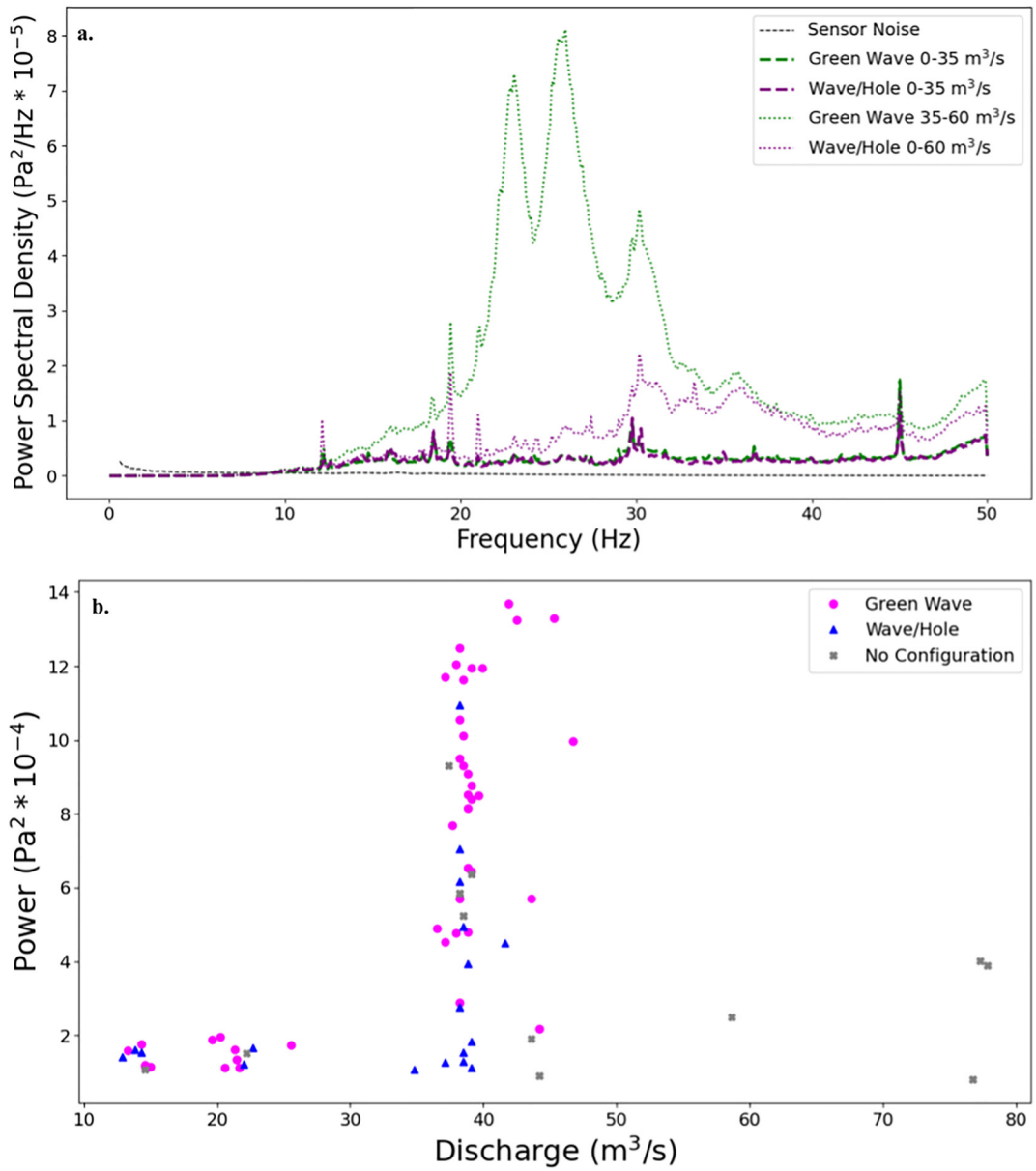

Figure 4. (a) Median power spectra of different wave types in 2022, with flow above and below the 35 m^3/s threshold, compared to the self-noise of the infrasound logger. (b) Plot of discharge versus power with different wave morphologies shown. In both analyses, no trends or dependence on wave configuration is observed below 35, but above 35 m^3/s green wave configuration is more powerful than wave/hole configuration.

3 years recorded, spanning a variety of discharge values. It is important to note that while monitorable sound only occurs above ~35 m^3/s, days with the highest discharge were not necessarily days with the highest infrasound power.

4.2. Daily Changes and Wave Configuration

Based on our observations of daily changes during periods of monitorable infrasound, Green Wave and Wave/Hole configurations at Boise Whitewater Park can change sound in a way that is consistent within a given year but does not necessarily persist over multiple years. This is shown during the first week of May 2016 (3 to 10 May) (Figures 5a and 5b), and June–July 2022 (19 to 26 June; 13 to 19 July) (Figures 6j and 6k), when wave configuration and infrasound had an observable pattern. Importantly, both periods occurred at discharge between

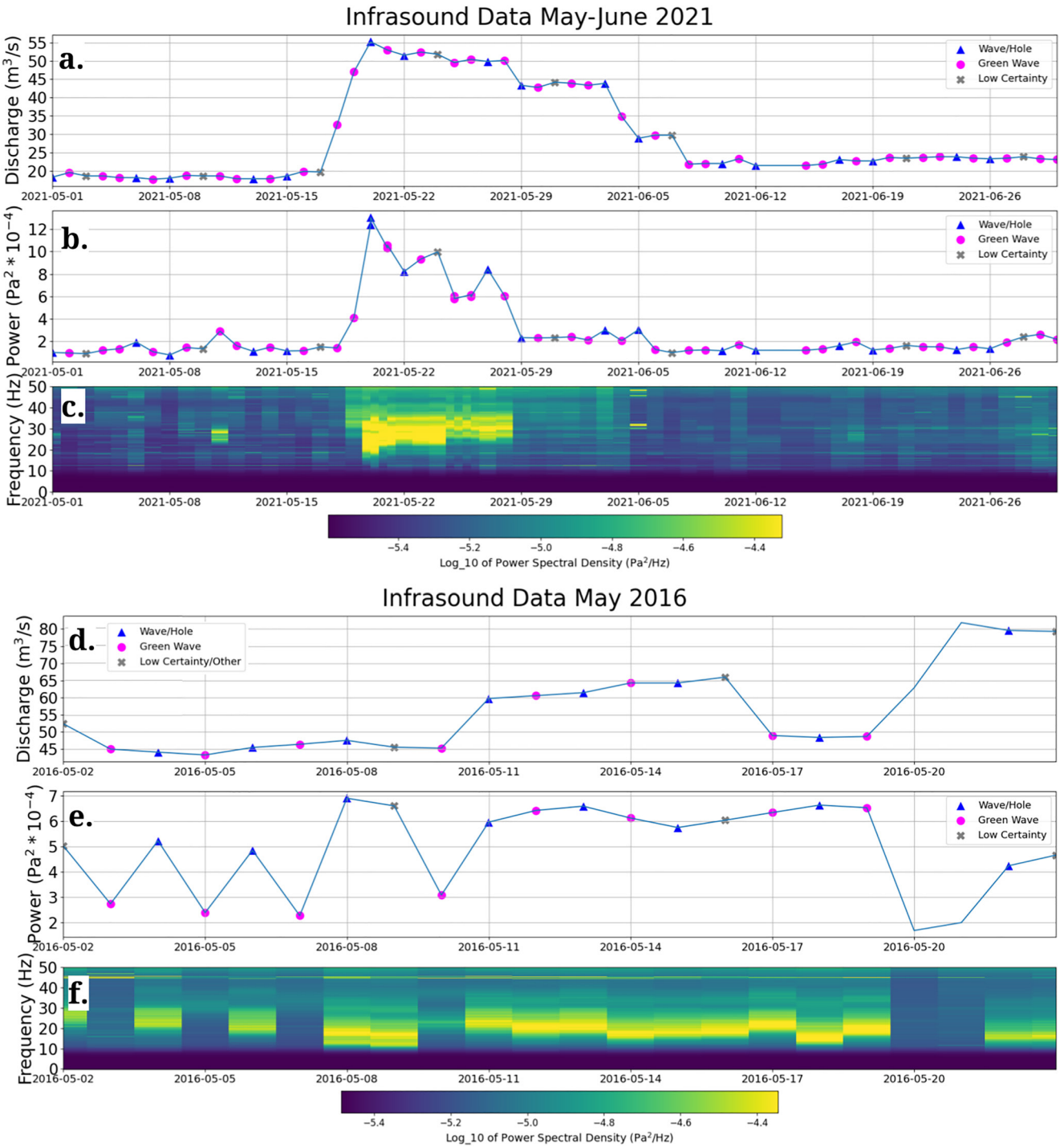

Figure 5. (a, d) Discharge, (b, e) Power, and (c, f) Frequency of stream and infrasound data recorded in June 2021 and May 2016.

35 (the threshold required for sound production) and 60 m^3/s (above which the normal dam configurations must be modified to ensure user safety). The unexpected reversal of the dependence of infrasound power on wave configuration between 2016 (in which Wave/Holes are louder), 2021 (in which the waves are indistinguishable), and 2022 (in which Green Waves are louder) shows that the flow characteristics that determine infrasound generation do not depend directly on the intended recreational use of the wave (i.e., its retentiveness), but are instead changed incidentally by dam reconfiguration. Morphological differences in the dam and riverbed between 2016 and 2022 (the strongest of which was caused by high discharge and precipitation in the spring of 2017), as well

10.1029/2023WR034554

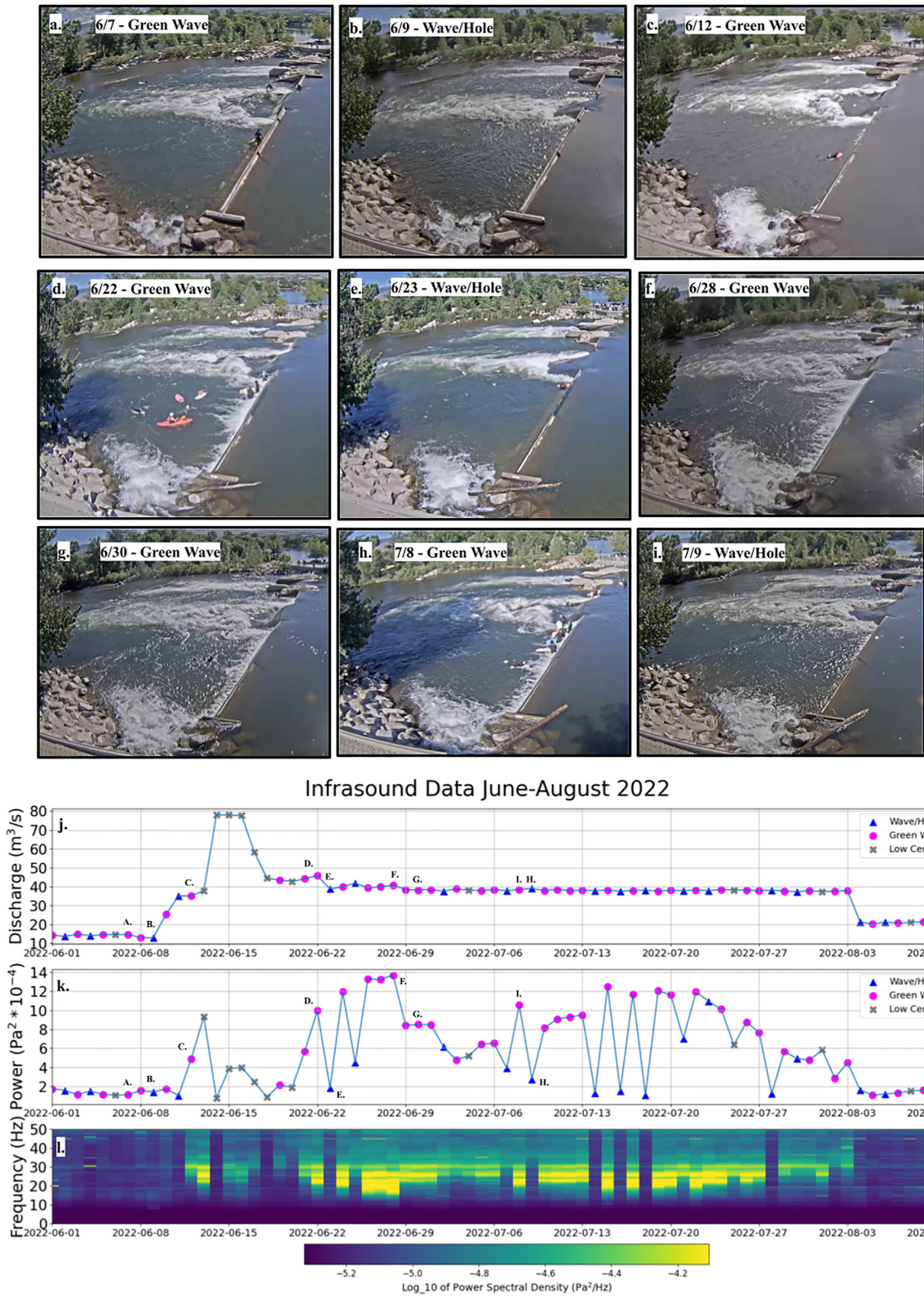

Figure 6. (a–i) Images and (j) Discharge, (k) Power, and (l) Spectrogram of stream and infrasound data during 2022. Conditions shown include Green Wave and Wave/Hole configurations occurring during a period of low discharge (~15 m^3/s) (a, b), a Green Wave configuration occurring at a higher discharge (~35 m^3/s) (c), medium sound power Green Wave configuration and low power Wave/Hole occurring at a similar discharge (~35–40 m^3/s) (d, e, h, and i), and days where infrasound power decreases despite unchanging discharge and no visible change to wave configuration (~40 m^3/s) (f, g).

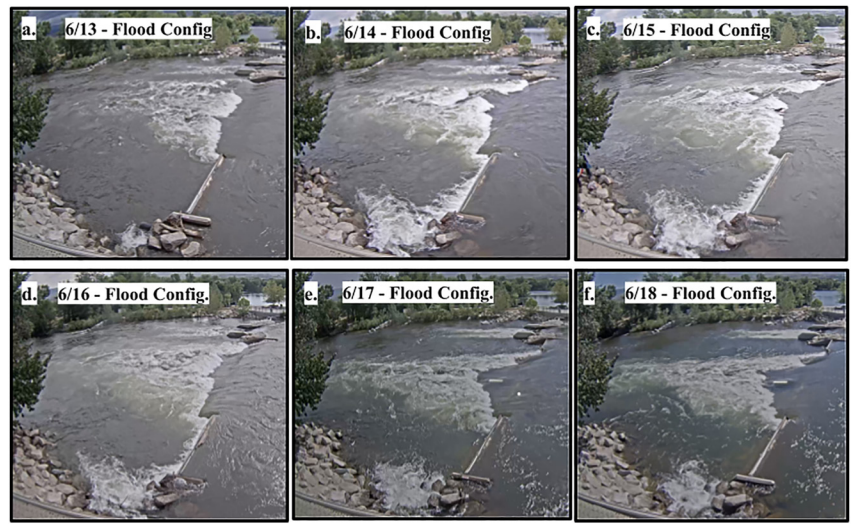

Figure 7. Photos of Boise Whitewater Park Phase 1 during flood configuration days (13–18 June 2022) when, due to high flow, the park had to use atypical settings to create recreational features while still meeting irrigation and safety standards. Flood configurations are identified by more open flashboards than normal Green Wave or Wave/Hole configurations. Images (a, d) show an open flashboard configuration without any additional significant features. Images (b, c) show an open flashboard configuration with Green Wave features and images (e, f) shows an open flashboard configuration with Wave/Hole features.

as changes in dam operator practices in how they adjust the dam to create appealing waves, may explain the year-to-year inconsistency (City of Boise, 2022; Stuebner, 2021).

When discharge reaches levels around ~60 m^3/s, BWPP1 widens the central wave by opening more flashboards. Some flood configurations mimicked traits of typical Green Wave and Wave/Hole forms for a larger volume of water (evidenced by some images during this period, (Figure 7)), while others formed a smooth non-wave. This means that for the highest periods of discharge within our study, the wave configuration was drastically altered from the usual schedule. Because of the inconsistency of these flood configurations, various acoustic effects may occur. Due to limited observations of high flow throughout the 3 years, we do not attempt to interpret higher flows.

4.3. The Origin of Whitewater Sounds and Future Work

Our work demonstrates that at favorable discharge levels, an adjustable whitewater feature produces monitorable infrasound under certain configurations and insignificant infrasound under different configurations. However, the enigmatic finding that the relationship between infrasound and wave morphology can disappear (2021) or reverse between years (2016 vs. 2022) highlights the need to identify the specific wave process responsible for low-frequency sound production. Clearly, the shape of the wave's front (the key characteristic manipulated by park staff for recreational utility) is not the sole determinant of the infrasound; otherwise, the dependence of infrasound on wave configuration would be consistent every year. We generally expect whitewater sounds to originate in violent regions of the flow (where tractions exerted on the atmosphere are strong) and/or foamy (where underwater sound transmits better to the atmosphere due to the smaller contrast in acoustic impedance). Breaking waves–either the main front of a wave (e.g., this study's Wave/Hole in 2016 and 2021) or secondary breakers downstream (e.g., this study's Green Wave in 2021–2022)–may serve as sound sources whose loudness can change dramatically in response to apparently minor changes in flow patterns that can be caused by changes in dam configuration in reaction to changing discharge levels or changes in bed configuration caused by higher flows (such as high discharge events like 2017) (Stuebner, 2021).

Though less prominent and smaller in discharge than the main wave feature, we also consider whether flow elsewhere along the dam could account for the observed low-frequency sound. Apart from the main wave, significant whitewater features along the dam include the rocky spillway on the river-left side, the bypass on the river-right side, and small waterfalls over raised flashboards (Figures 6a–6i). Although we note that these features are less

likely to be major sources of infrasound based on their morphology (Section 2.1), flow through all of these features depends on the difference between the upstream and downstream water levels, which we note is consistently higher for Green Waves than for Wave/Hole configuration. We acknowledge that changes to the main wave may incidentally increase or decrease flow in other parts of the dam whose morphology is more conducive to infrasound production; therefore, future work may elucidate morphological controls on whitewater infrasound production using high-resolution acoustic or optical imaging to identify source regions, or by direct manipulation of the dam to identify morphological changes that coincide with increasing infrasound power. In particular, during the period examined in 2022, the upstream water level only rises above raised flashboards when the dam is configured for a green wave. During late June and early July 2022, most green waves were accompanied by flashboard spillover (Figures 6d, 6f, 6g, and 6h). This specific time period contained higher infrasound power, but we were unable to identify whether the source was from higher discharge, the presence of flashboard spillover, or a compounding of the two factors. However, there are instances of green waves without spillover that create infrasound (e.g., Figure 6c) in early June, demonstrating that the waterfall is not required for green waves to create infrasound.

Finally, we affirm the utility of adjustable waves in whitewater parks for studying effects of hydrodynamics and discharge on geophysical wave fields (first demonstrated by Ronan et al. (2017)). These increasingly common waves offer the unique ability to manipulate wave morphology at river scale and can perform useful roles in controlled short-term experiments, as well as long-term natural experiments when the wave is routinely adjusted similar to this study.

5. Conclusions

In order to better understand sound dependence on discharge and wave configuration, this study examined infrasound from 3 years at an adjustable wave feature located in Boise Whitewater Park. In comparison to past research that investigated discharge and wave morphology separately, this study examines these variables jointly in their relationship with low-frequency sound. Discharge above a specific threshold was required for monitorable infrasound, where relationships between sound and wave configuration could only be discerned for discharge greater than 35 m^3/s. Morphological changes in the wave could cause sound to become powerful or insignificant; this could be the reason that changes in wave configuration and infrasound were consistent within the year but not between years. With the observations and analysis provided in this paper, there is evidence that infrasound is visibly related to fluvial wave morphology and that river morphology could have additional contributions. By using controlled settings like those found in whitewater parks, further collaboration offers opportunities for future work into the origin of whitewater sound. As more research is done into the application of infrasound in relation to measuring discharge and identifying hazardous waves, more opportunities arise to investigate the ways in which potential new applications can be used and where they are most effective.

Data Availability Statement

Data presented here is archived and may be accessed from the Boise State University Infrasound Data Repository at https://scholarworks.boisestate.edu/infrasound_data/ and https://doi.org/10.18122/infrasound_data.11.boisestate (Tatum & Anderson, 2022).

Acknowledgments
Thank you to Paul Primus for demonstrating and discussing management and mechanics of Boise Whitewater Park. Additional thanks to Scott Gauvain, Tamara Satterwhite, and Owen Walsh for assistance with fieldwork, recording, and data analysis. Finally, we are grateful for thorough and insightful reviews by John Lyons and two anonymous reviewers. This project was funded by NSF award number EAR-2051670.

References

Anderson, J. F., Johnson, J. B., Bowman, D. C., & Ronan, T. J. (2018). The gem infrasound logger and custom-built instrumentation. *Seismological Research Letters*, *89*(1), 153–164. https://doi.org/10.1785/0220170067

Arrowsmith, S. J., & Hedlin, M. A. H. (2005). Observations of infrasound from surf in southern California. *Geophysical Research Letters*, *32*(9), L09810. https://doi.org/10.1029/2005GL022761

Asiaban, P., Rennie, C. D., & Egsgard, N. (2021). Sensitivity analysis of adjustable river surf waves in the absence of channel drop. *Water*, *13*(9), 1287. https://doi.org/10.3390/w13091287

Bedard, A., & Georges, T. (2000). Atmospheric infrasound. *Acoustics Australia*, *28*(2), 47–52. https://doi.org/10.1063/1.883019

Bosa, A., Johnson, J., De Angelis, S., Lyons, J., Roca, A., Anderson, J., & Pineda, A. (2021). Tracking secondary lahar flow paths and characterizing pulses and surges using infrasound array networks at Volcán de Fuego, Guatemala. *Volcanica*, *4*(2), 239–256. https://doi.org/10.30909/vol.04.02.239256

Brown, D., Ceranna, L., Prior, M., Mialle, P., & Le Bras, R. J. (2014). The IDC seismic, hydroacoustic and infrasound global low and high noise models. *Pure and Applied Geophysics*, *171*(3–5), 361–375. https://doi.org/10.1007/s00024-012-0573-6

Che, I. Y., Park, J., Kim, I., Kim, T. S., & Lee, H. I. (2014). Infrasound signals from the underground nuclear explosions of North Korea. *Geophysical Journal International*, *198*(1), 495–503. https://doi.org/10.1093/gji/ggu150

Chow, T. (1959). Open-channel hydraulics. *Caldwell*.

City of Boise. (2022). *J.A. and Kathryn Albertson family foundation Boise whitewater Park*. City of Boise. Retrieved from https://www.cityofboise.org/departments/parks-and-recreation/parks/ja-and-kathryn-albertson-family-foundation-boise-whitewater-park/

De Padova, D., Mossa, M., & Sibilla, S. (2017). SPH modelling of hydraulic jump oscillations at an abrupt drop. *Water*, *9*(10), 790. https://doi.org/10.3390/w9100790

Fekete, B. M., & Vörösmarty, C. J. (2007). The current status of global river discharge monitoring and potential new technologies complementing traditional discharge measurements. *IAHS Publcation*, *309*, 129–136.

Gochis, D., Schumacher, R., Friedrich, K., Doesken, N., Kelsch, M., Sun, J., et al. (2015). The great Colorado flood of September 2013. *Bulletin of the American Meteorological Society*, *96*(9), 1461–1487. https://doi.org/10.1175/BAMS-D-13-00241.1

Hannah, D. M., Demuth, S., van Lanen, H. A., Looser, U., Prudhomme, C., Rees, G., et al. (2011). Large-scale river flow archives: Importance, current status and future needs. *Hydrological Processes*, *25*(7), 1191–1200. https://doi.org/10.1002/hyp.7794

Hübl, J., Schimmel, A., Kogelnig, A., Suriñach, E., Vilajosana, I., & McArdell, B. W. (2013). A review on acoustic monitoring of debris flow. *International Journal of Safety and Security Engineering*, *3*(2), 105–115. https://doi.org/10.2495/safe-v3-n2-105-115

Johnson, J. B., Anderson, J. F., Marshall, H. P., Havens, S., & Watson, L. M. (2021). Snow avalanche detection and source constraints made using a networked array of infrasound sensors. *Journal of Geophysical Research: Earth Surface*, *126*(3), e2020JF005741. https://doi.org/10.1029/2020jf005741

Johnson, J. B., Lees, J. M., & Yepes, H. (2006). Volcanic eruptions, lightning, and a waterfall: Differentiating the menagerie of infrasound in the Ecuadorian jungle. *Geophysical Research Letters*, *33*(6), L06308. https://doi.org/10.1029/2005GL025515

Johnson, J. B., & Palma, J. L. (2015). Lahar infrasound associated with Volcán Villarrica's 3 March 2015 eruption. *Geophysical Research Letters*, *42*(15), 6324–6331. https://doi.org/10.1002/2015gl065024

Leutheusser, H. J., & Birk, W. M. (1991). Drownproofing of low overflow structures. *Journal of Hydraulic Engineering*, *117*(2), 205–213. https://doi.org/10.1061/(ASCE)0733-9429(1991)117:2(205)

Lyons, J. J., Dietterich, H. R., Patrick, M. P., & Fee, D. (2021). High-speed lava flow infrasound from Kīlauea's fissure 8 and its utility in monitoring effusion rate. *Bulletin of Volcanology*, *83*(11), 66. https://doi.org/10.1007/s00445-021-01488-7

Osborne, W. A., Hodge, R. A., Love, G. D., Hawkin, P., & Hawkin, R. E. (2021). Babbling brook to thunderous torrent: Using sound to monitor river stage. *Earth Surface Processes and Landforms*, *46*(13), 2656–2670. https://doi.org/10.1002/esp.5199

Ronan, T. J., Lees, J. M., Mikesell, D. T., Anderson, J. F., & Johnson, J. B. (2017). Acoustic and seismic fields of hydraulic jumps at varying Froude numbers. *Geophysical Research Letters*, *44*(19), 9734–9741. https://doi.org/10.1002/2017gl074511

Schmandt, B., Aster, R. C., Scherler, D., Tsai, V. C., & Karlstrom, K. (2013). Multiple fluvial processes detected by riverside seismic and infrasound monitoring of a controlled flood in the Grand Canyon. *Geophysical Research Letters*, *40*(18), 4858–4863. https://doi.org/10.1002/grl.50953

Stuebner, S. (2021). *Part 4: Snowmageddon 2017 – 101 Days of flooding on the Boise River*. Boise River. Retrieved from https://boiseriver.org/history/

Tatum, T., & Anderson, J. (2022). Dataset for Whitewater Sound Dependence on Discharge and Wave Configuration at an Adjustable Wave Feature. *Boise State University Infrasound Data Repository*, 11. Retrieved from https://scholarworks.boisestate.edu/infrasound_data/11

U.S. Geological Survey. (2016). National water information system data available on the world wide web (USGS water data for the nation). Retrieved from https://waterdata.usgs.gov/monitoring-location/13206000/#parameterCode=00060&startDT=2021-03-12&endDT=2021-07-15

Watson, L. M., Iezzi, A. M., Toney, L., Maher, S. P., Fee, D., McKee, K., et al. (2022). Volcano infrasound: Progress and future directions. *Bulletin of Volcanology*, *84*(5), 44. https://doi.org/10.1007/s00445-022-01544-w

References From the Supporting Information

Boise Whitewater Park. (2022). *Posts*. Facebook. Retrieved from https://www.facebook.com/boiseriverpark/